

# Evolving to learn: discovering interpretable plasticity rules for spiking networks

Jakob Jordan<sup>\*1</sup>, Maximilian Schmidt<sup>\*2,3</sup>, Walter Senn<sup>1</sup>, and Mihai A. Petrovici<sup>1,4</sup>

<sup>1</sup>Department of Physiology, University of Bern, Bern, Switzerland

<sup>2</sup>Ascent Robotics, Tokyo, Japan

<sup>3</sup>RIKEN Center for Brain Science, Tokyo, Japan

<sup>4</sup>Kirchhoff-Institute for Physics, Heidelberg University, Heidelberg, Germany

## Abstract

Continuous adaptation allows survival in an ever-changing world. Adjustments in the synaptic coupling strength between neurons are essential for this capability, setting us apart from simpler, hard-wired organisms. How these adjustments come about is essential both for understanding biological information processing and for developing cognitively performant artificial systems. We suggest an automated approach for finding biophysically plausible plasticity rules based on the definition of task families, associated performance measures and biophysical constraints. This approach makes the relative weighting of guiding factors explicit, explores large search spaces, encourages diverse sets of hypotheses, and can discover domain-specific solutions. By evolving compact symbolic expressions we ensure the discovered plasticity rules are amenable to intuitive understanding. This is fundamental for successful communication and human-guided generalization, for example to different network architectures or task domains. We demonstrate the flexibility of our approach by discovering efficient plasticity rules in typical learning scenarios.

**Keywords:** metalearning, learning to learn, synaptic plasticity, spiking neuronal networks, genetic programming

## 1 Introduction

How do we learn? Whether we are memorizing the way to the lecture hall at a conference or mastering a new sport, somehow our central nervous system is able to retain the relevant information over extended periods of time, sometimes with ease, other times only after intense practice. This acquisition of new memories and skills manifests at various levels of the system, with changes of the interaction strength between neurons being a key ingredient. Uncovering the mechanisms behind this synaptic plasticity is a key challenge in understanding brain function. Most studies approach this monumental task by searching for symbolic expressions that map local biophysical quantities to changes of the connection strength between cells (Fig. 1A, B).

Approaches to deciphering synaptic plasticity can be broadly categorized into bottom-up and top-down. Bottom-up approaches typically rely on experimental data (e.g., [Artola et al., 1990](#); [Dudek and Bear, 1993](#); [Bi and Poo, 1998](#); [Ngezahayo et al., 2000](#)) to derive dynamic equations for synaptic parameters that lead to functional emergent macroscopic behavior if appropriately embedded in networks (e.g., [Gütig et al., 2003](#); [Izhikevich, 2007](#); [Clopath et al., 2010](#)). Top-down approaches proceed in the opposite direction: from a high-level description of network function, e.g., in terms of an objective function (e.g., [Toyoizumi et al., 2005](#); [Deneve, 2008](#); [Kappel et al., 2015](#); [Kutschireiter et al., 2017](#); [Sacramento et al., 2018](#); [Göltz et al., 2019](#)), dynamic equations for synaptic changes are derived and biophysically plausible implementations suggested. Evidently, this demarcation is not strict, as most approaches seek some balance between experimental evidence,

<sup>\*</sup>These authors contributed equally to this work.

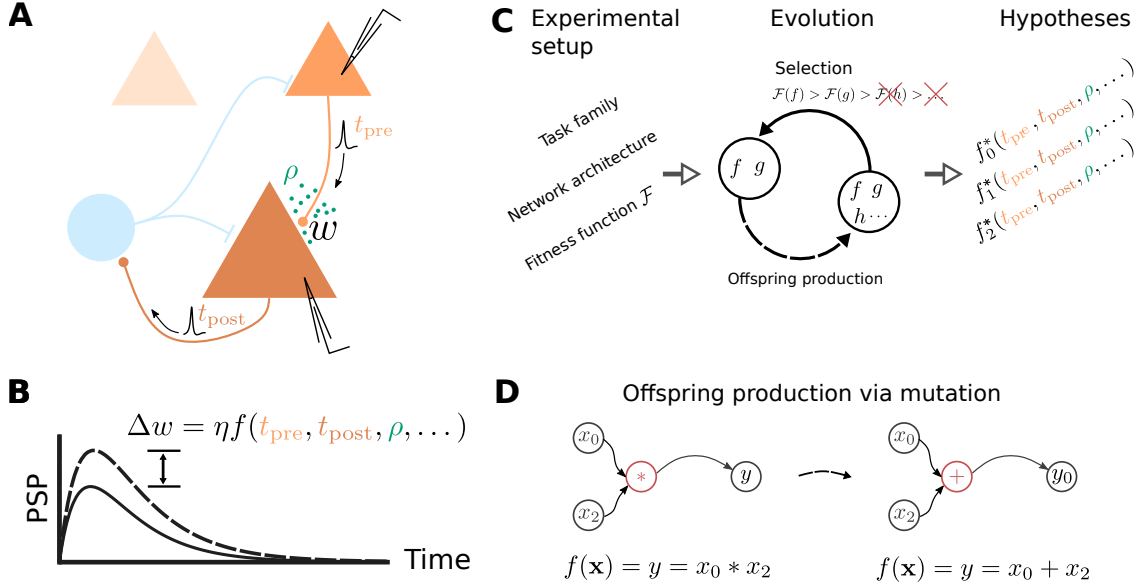


**Figure 1: Artificial evolution of synaptic plasticity rules in spiking neuronal networks.** (A) Sketch of cortical microcircuits consisting of pyramidal cells (orange) and inhibitory interneurons (blue). Stimulation elicits action potentials in pre- and postsynaptic cells, which, in turn, influence synaptic plasticity. (B) Synaptic plasticity leads to a weight change ( $\Delta w$ ) between the two cells, here measured by the change in the amplitude of post-synaptic potentials. The change in synaptic weight can be expressed by a function  $f$  that in addition to spike timings ( $t_{pre}, t_{post}$ ) can take into account additional local quantities, such as the concentration of neuromodulators ( $\rho$ , green dots in A) or postsynaptic membrane potentials. (C) For a specific experimental setup, an evolutionary algorithm searches for individuals representing functions  $f$  that maximize the corresponding fitness function  $\mathcal{F}$ . An offspring is generated by modifying the genome of a parent individual. Several runs of the evolutionary algorithm can discover phenomenologically different solutions ( $f_0, f_1, f_2$ ) with comparable fitness. (D) An offspring is generated from a single parent via mutation. Mutations of the genome can, for example, exchange mathematical operators, resulting in a different function  $f$ .

functional considerations and model complexity. However, the relative weighting of each of these aspects is usually not made explicit in the communication of scientific results, making it difficult to track by other researchers. Furthermore, the selection of specific tasks to illustrate the effect of a suggested learning rule is usually made only after the rule was derived based on other considerations. Hence, this typically does not consider competing alternative solutions, as an exhaustive comparison would require significant additional investment of human resources. A related problem is that researchers, in a reasonable effort to use resources efficiently, tend to focus on promising parts of the search space around known solutions, leaving large parts of the search space unexplored (Radi and Poli, 2003).

We suggest an automated approach to discover learning rules in spiking neuronal networks that explicitly addresses these issues. Automated procedures interpret the search for biological plasticity mechanisms as an optimization problem (Bengio et al., 1992), an idea typically referred to as meta-learning or learning-to-learn. These approaches make the emphasis of particular aspects that guide this search explicit and place the researcher at the very end of the process, supporting much larger search spaces and the generation of a diverse set of hypotheses. Furthermore, they have the potential to discover domain-specific solutions that are more efficient than general-purpose algorithms. Early experiments focusing on learning in artificial neural networks (ANNs) made use of gradient descent or genetic algorithms to optimize parameterized learning rules (Bengio et al., 1990, 1992, 1993) or genetic programming to evolve less constrained learning rules (Bengio et al., 1994; Radi and Poli, 2003), rediscovering mechanisms resembling the backpropagation of errors (Ivakhnenko, 1971; Rumelhart et al., 1985). Recent experiments demonstrate how optimization methods can design optimization algorithms for recurrent ANNs (Andrychowicz et al., 2016).

We extend these meta-learning ideas to spiking neuronal networks. The discrete nature of spike-based neuronal interactions endows these networks with rich dynamical and functional properties (e.g., [Dold et al., 2019](#); [Jordan et al., 2019](#); [Keup et al., 2020](#)). In addition, with the advent of non-von Neumann computing systems based on spiking neuronal networks with online learning capabilities ([Moradi et al., 2017](#); [Davies et al., 2018](#); [Billaudelle et al., 2019](#)), efficient learning algorithms for spiking systems become increasingly relevant for non-conventional computing. Here, we employ genetic programming (Fig. 1C, D; [Koza, 2010](#)) as a search algorithm for two main reasons. First, genetic programming can operate on analytically tractable mathematical expressions describing synaptic weight changes that are interpretable. Second, an evolutionary search does not need to compute gradients in the search space, thereby circumventing the need to estimate a gradient in non-differentiable systems.

We apply our approach to three different learning paradigms for spiking neuronal networks: reward-driven, error-driven and correlation-driven learning. We discover efficient plasticity rules for these task families that perform competitively with known solutions. For the reward-driven task, we reliably reproduce a previously suggested solution that achieves high performance. In the error-driven learning scenario, the evolutionary search discovers a variety of solutions which, with appropriate analysis of the corresponding expressions, can be shown to effectively implement stochastic gradient descent. Finally, in the correlation-driven task, our method generates various hypotheses for STDP-like plasticity rules with diverse weight dynamics that match the performance of a rule derived under optimality considerations. Our results demonstrate the significant potential of automated procedures in the search for plasticity rules in spiking neuronal networks, analogous to the transition from hand-designed to learned features that lies at the heart of modern machine learning.

## 2 Results

### 2.1 Setting up an evolutionary search for plasticity rules

We introduce the following recipe to search for biophysically plausible plasticity rules in spiking neuronal networks. First we determine a task family of interest and an associated experimental setup which includes specification of the network architecture, e.g., neuron types and connectivity, as well as stimulation protocols or training data sets. Crucially, this step involves defining a fitness function to guide the evolutionary search towards promising regions of the search space. It assigns high fitness to those individuals, i.e., learning rules, that solve the task well and low fitness to others. The fitness function may additionally contain constraints implied by experimental data or arising from computational considerations. We determine each individual's fitness on various examples from the given task family, e.g., different input spike train realizations, to discover plasticity rules that generalize well ([Chalmers, 1991](#); [Soltoggio et al., 2018](#)). Finally, we specify the neuronal variables available to the plasticity rule, such as low-pass-filtered traces of pre- and postsynaptic spiking activity or neuromodulator concentrations. This choice is guided by biophysical considerations, e.g., which quantities are locally available at a synapse, as well as by the task family, e.g., whether reward or error signals are provided by the environment. We write the plasticity rule in the general form  $\Delta w = \eta f(\dots)$ , where  $\eta$  is a fixed learning rate, and employ an evolutionary search to discover functions  $f$  that lead to high fitness.

We propose to use genetic programming (GP) as an evolutionary algorithm to discover plasticity rules in spiking neuronal networks. GP applies mutations and selection pressure to an initially random population of computer programs to artificially evolve algorithms with desired behaviors (e.g., [Koza, 1992, 2010](#)). Here we consider the evolution of mathematical expressions. We employ a specific form of GP, Cartesian genetic programming (CGP; e.g. [Miller and Thomson, 2000](#); [Miller, 2011](#)), that uses an indexed graph representation of programs. The genotype of an individual is a two-dimensional Cartesian graph (Fig. 2A, top). Over the course of an evolutionary run, this graph has a fixed number of input, output, and internal nodes. The operation of each internal node is fully described by a single function gene and a fixed number of input genes. A function table maps function genes to mathematical operations (Fig. 2A, bottom), while input genes determine from where this node receives data. A given genotype is decoded into a corresponding computational graph (the phenotype, Fig. 2B) which defines a function  $f$ . During the evolutionary run, mutations

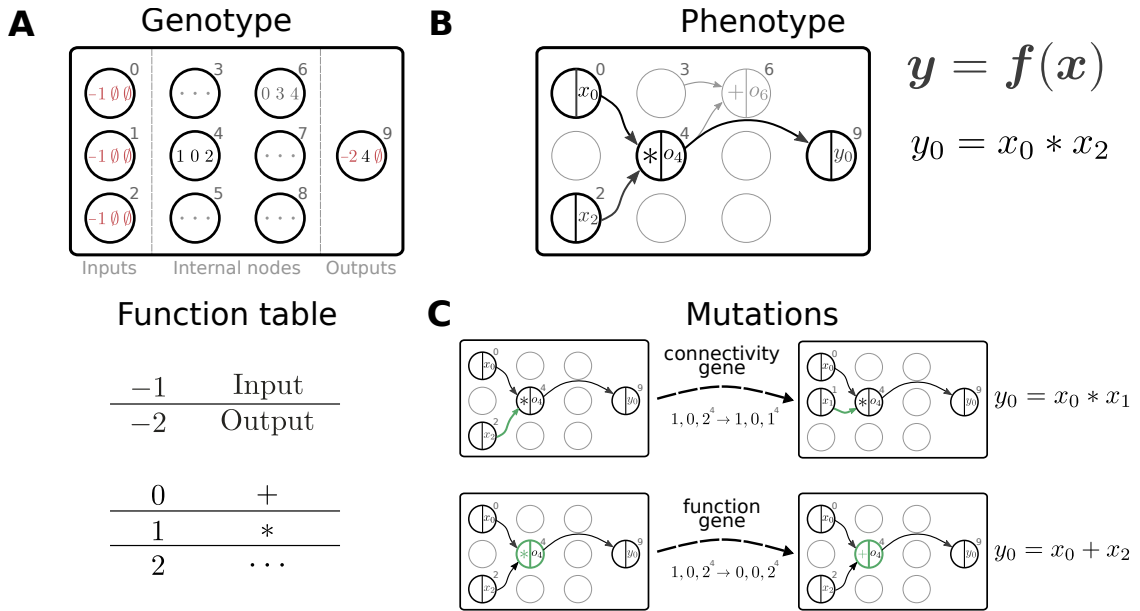


Figure 2: **Representation and mutation of mathematical expressions in Cartesian genetic programming.** (A) The genotype of an individual is a two-dimensional Cartesian graph (top). In this example, the graph contains three input nodes (0 – 2), six internal nodes (3 – 8) and a single output node (9). In each node the genes of a specific genotype are shown, encoding the operator used to compute the node’s output and its inputs. Each operator gene maps to a specific mathematical function (bottom). Special values (−1, −2) represent input and output nodes. For example, node 4 uses the operator 1, the multiplication operation “\*”, and receives input from nodes 0 and 2. This node’s output is hence given by  $x_0 * x_2$ . The number of input genes per node is determined by the operator with the maximal arity (here two). Red genes highlight fixed genes that can not be mutated.  $\emptyset$  denotes non-coding genes. (B) The computational graph (phenotype) generated by the genotype in A. Input nodes ( $x_0, x_1, x_2$ ) represent the arguments of the function  $f$ . Each output node selects one of the other nodes as a return value of the computational graph, thus defining a function from input  $\mathbf{x}$  to output  $\mathbf{y} = f(\mathbf{x})$ . Here, the output node selects node 4 as a return value. Some nodes defined in the genotype are not used by a particular realization of the computational graph (light gray nodes, e.g., node 6). (C) Mutations in the genome either lead to a change in graph connectivity (top, green arrow) or alter the operators used by an internal node (bottom, green node). Mutations that do not affect the phenotype, e.g., in node 6, are called silent mutations. Here, both mutations affect the phenotype and are hence not silent.

of the genotype alter connectivity and node operations, which can modify the encoded function (Fig. 2C). The indirect encoding of the computational graph via the genotype supports variable-length phenotypes, since some internal nodes may not be used to compute the output (Fig. 2B). The size of the genotype, in contrast, is fixed, thereby restricting the maximal size of the computational graph and ensuring compact, interpretable mathematical expressions. Furthermore, the separation into genotype and phenotype allows for “silent mutations”, i.e., mutations in the genotype that do not alter the phenotype. These silent mutations can lead to more efficient search as they can accumulate and in combination lead to an increase in fitness once affecting the phenotype (Miller and Thomson, 2000). A  $\mu + \lambda$  evolution strategy (Beyer and Schwefel, 2002) drives evolution by creating the next generation of individuals from the current one via tournament selection, mutation and selection of the fittest individuals (Sec. 4.1). Prior to starting the search, we choose the mathematical operations that can appear in the plasticity rule and other (hyper)parameters of the Cartesian graph and evolutionary algorithm. For simplicity, we consider a restricted set of mathematical operations and additionally make use of nodes with constant output. After the search has completed, e.g., by reaching a target fitness value or a maximal number of generations, we

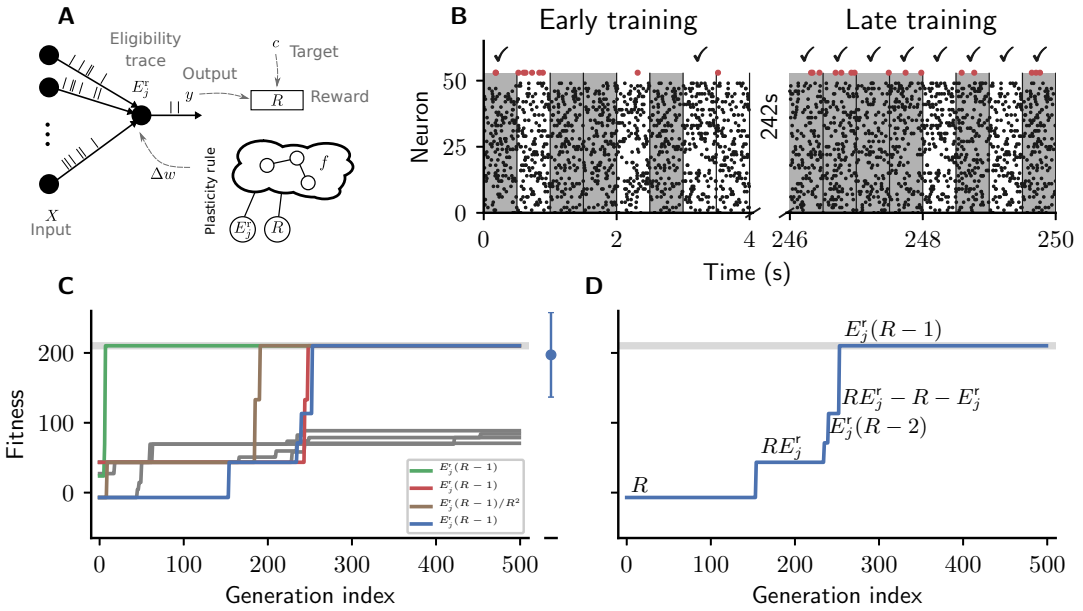


Figure 3: **Cartesian genetic programming evolves an efficient reward-driven learning rule.** (A) Network sketch. Multiple input neurons with Poisson activity project to a single output unit. Pre- and postsynaptic activity generate an eligibility trace in each synapse. Comparison between the output activity and the target activity generates a reward signal. Both of these are provided to the plasticity rule that determines the weight update. (B) Raster plot of the activity of input neurons (small black dots) and output neuron (large red dots). Gray (white) background indicate patterns for which the output should be active (inactive). Check marks indicate correct classifications. We show 8 trials at the beginning (left) and the end of training (right) using the evolved plasticity rule:  $\Delta w_j = \eta E_j^r(T)(R - 1)$ . (C) Fitness of best individual per generation as a function of the generation index for multiple runs of the evolutionary algorithm with different initial conditions. Labels represent the rule at the end of the respective run for the four runs with the highest final fitness (colored lines). Dark gray lines represent runs with low final fitness. Light gray line indicates the fitness of Eq. 2. Blue marker with error bars represents fitness of the discovered rule  $\Delta w_j = \eta E_j^r(T)(R - 1)$  on 10 validation tasks not used during the evolutionary search. (D) Function  $f$  encoded in the best individual as a function of the generation index for one run of the evolutionary algorithm. Expressions are only shown after the generation in which a change in highest fitness occurred.

analyze the discovered set of solutions.

In the following, we describe the results of three experiments following the recipe outlined above.

## 2.2 Evolving an efficient reward-driven plasticity rule

We consider a reinforcement-learning task for spiking neurons similar to [Urbanczik and Senn \(2009\)](#). The experiment can be succinctly described as follows:  $N$  inputs project to a single readout modeled by a leaky integrator neuron with exponential postsynaptic currents and stochastic spike generation (for details see Sec. 4.5). We generate a finite number  $M$  of frozen-Poisson-noise patterns of duration  $T$  and assign each of these randomly to one of two classes. The output neuron should learn to classify each of these spatio-temporal input patterns into the corresponding class using a spike/no-spike code (Fig. 3A, B).

The fitness  $\mathcal{F}(f)$  of an individual encoding the function  $f$  is measured by the average cumulative

reward obtained over a certain number of experiments  $n_{\text{exp}}$ , each consisting of  $n$  classification tasks:

$$\mathcal{F}(f) := \frac{1}{n_{\text{exp}}} \sum_{k=1}^{n_{\text{exp}}} R_k(f), \quad (1)$$

where  $R_k(f) = \sum_{i=1}^n R_{k,i}(f)$  is the cumulative reward obtained in experiment  $k$ . The reward  $R_{k,i}$  is 1 if the classification is correct and  $-1$  otherwise. Each experiment contains different realizations of frozen-noise input spike trains with associated class labels.

[Urbanczik and Senn \(2009\)](#) derive a plasticity rule that allows the output neuron to solve the task from repeated presentation of patterns:

$$\Delta w_j = \eta E_j^r(t)(R - 1). \quad (2)$$

Here  $\eta$  represents a fixed learning rate, and  $j$  represents the presynaptic neuron index.  $E_j^r$  is an eligibility trace that contains contributions from the spiking activity of pre- and post-synaptic neurons which is updated over the course of a single trial (for details see Sec. 4.5). Similarly to [Urbanczik and Senn \(2009\)](#), reward and eligibility trace values at the end of each trial ( $t = T$ ) are used to determine synaptic weight changes. The plasticity rule can be written in the following general form where, for comparability, we choose the same learning rate as for the original rule (Eq. 2):

$$\Delta w_j = \eta f(R, E_j^r(T)). \quad (3)$$

Using CGP with two inputs  $(R, E_j^r(T))$  we search for plasticity rules that maximize the fitness  $\mathcal{F}(f)$  (Eq. 1).

In about half of the runs the the evolutionary algorithm evolves a plasticity rule identical to the one derived in previous work (Eq. 2), which achieves high fitness (Fig. 3C). As the reward is constrained to  $R \in \{-1, 1\}$  the task includes a degeneracy and different functions  $f$  can lead to identical weight changes. Some of these phenomenologically identical expressions were found by the evolutionary algorithm, such as  $E_j^r(R - 1) \frac{1}{R^2}$ ,  $RE_j^r(1 - R)$ ,  $-E_j^r + \frac{E_j^r}{R}$ . An essential benefit of our approach is that we can identify such classes of solutions that lead to identical weight changes thanks to a crucial property of genetic programming: since we obtain analytically tractable expressions for the plasticity rule, we can analyze them with conventional methods, in contrast to approaches representing plasticity rules with ANNs (e.g., [Risi and Stanley, 2010](#); [Orchard and Wang, 2016](#); [Bohnstingl et al., 2019](#)), for which it is challenging to fully understand their macroscopic computation. A further advantage of obtaining analytical expressions is the possibility to interpret the evolutionary steps by which the search progresses. We observe that already after a few generations the algorithm discovers an important basic ingredient for learning from rewards: the factor  $RE_j^r$  (Fig. 3D). This product, for example, increases weights of projections which have contributed to the correct spiking of the output neuron, causing these neurons to be even more active the next time this specific pattern is encountered. However, this rule is not stable: due to randomness in spike generation, weight changes do not subside even if the neuron always responds correctly and can thus lead to unlearning of good weight configurations. Over the next few hundred generations, refinements of this solution evolve without losing the basic structure (Fig. 3D). Finally, a stable solution for this task is found: evolution discovers that weights should only change if the classification was wrong and remain unchanged if it was correct, i.e., the product is replaced by  $E_j^r(R - 1)$ .

In conclusion, the evolutionary search discovers an efficient learning rule for the considered reinforcement learning task. As we obtain it in interpretable form, we can identify it with a previously suggested, human-designed plasticity rule and analyze how different functions can lead to identical weight changes.

### 2.3 Evolving an efficient error-driven plasticity rule

We next consider a supervised learning task in which a neuron receives information about how far its output is from the desired behavior, instead of just a scalar reward signal as in the previous task. The widespread success of this approach in machine learning highlights the efficacy of learning

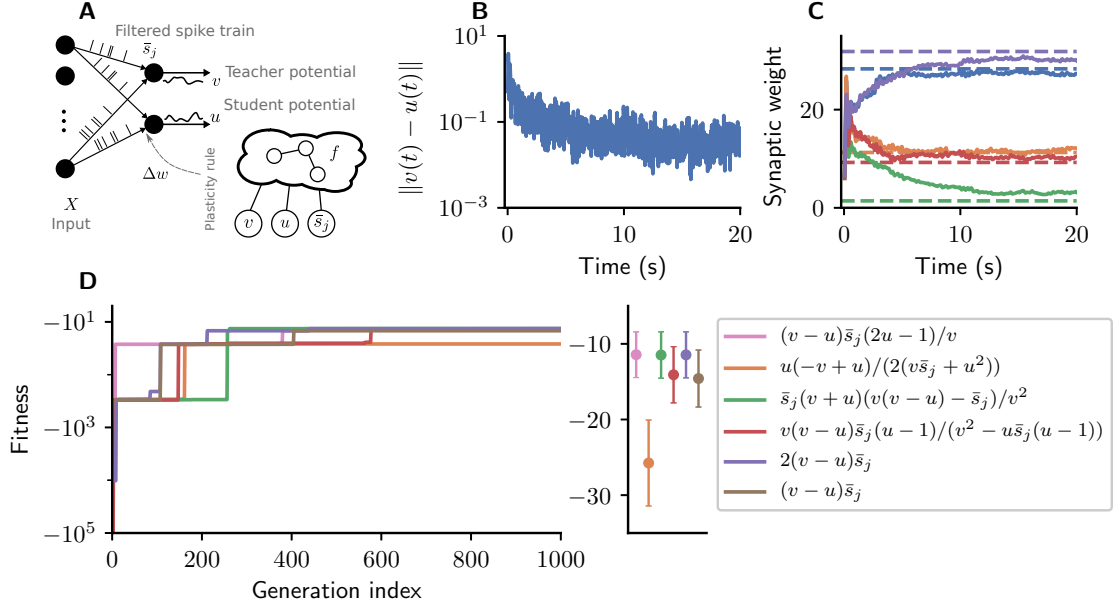


**Figure 4: Cartesian genetic programming evolves efficient error-driven learning rules.** **(A)** Network sketch. Multiple input neurons with Poisson activity project to two neurons. One of the neurons (the teacher) generates a target for the other (the student). The membrane potentials of teacher and student as well as the filtered pre-synaptic spike trains are provided to the plasticity rule that determines the weight update. **(B)** Root mean squared error between the teacher and student membrane potential over the course of learning using the evolved plasticity rule:  $\Delta w_j(t) = \eta [v(t) - u(t)] \bar{s}_j(t)$ . **(C)** Synaptic weights over the course of learning corresponding to panel B. Horizontal dashed lines represent target weights, i.e., the fixed synaptic weights onto the teacher. **(D)** Fitness of the best individual per generation as a function of the generation index for multiple runs of the evolutionary algorithm with different initial conditions. Labels represent the rule at the end of the respective run. Colored markers with error bars represent fitness of the respective plasticity rule on 15 validation tasks not used during the evolutionary search.

from errors compared to correlation- or reward-driven learning (Goodfellow et al., 2016). It has therefore often been hypothesized that evolution has installed similar capabilities in biological nervous systems (see, e.g., Marblestone et al., 2016; Whittington and Bogacz, 2019).

Urbanczik and Senn (2014) introduce an efficient, flexible and biophysically plausible implementation of error-driven learning via multi-compartment neurons. For simplicity, we consider an equivalent formulation of this learning principle in terms of two point neurons modeled as leaky integrator neurons with exponential postsynaptic currents and stochastic spike generation. One neuron mimics the somatic compartment and provides a teaching signal to the other neuron acting as the dendritic compartment. Here, the difference between the teacher and student membrane potentials drives learning:

$$\Delta w_j(t) = \eta [v(t) - u(t)] \bar{s}_j(t), \quad (4)$$

where  $v$  is the teacher potential,  $u$  the student membrane potential, and  $\eta$  a fixed learning rate.  $\bar{s}_j(t) = (\kappa * s_j)(t)$  represents the the presynaptic spike train  $s_j$  filtered by the synaptic kernel  $\kappa$ . Eq. 4 can be interpreted as stochastic gradient descent on an appropriate cost function (Urbanczik and Senn, 2014) and can be extended to support credit assignment in hierarchical neuronal networks (Sacramento et al., 2018). For simplicity we assume the student has direct access to the teacher's membrane potential, but in principle one could also employ proxies such as firing rates as suggested in Pfister et al. (2010); Urbanczik and Senn (2014).

We consider a one-dimensional regression task in which we feed random Poisson spike trains into the two neurons (Fig. 4A). The teacher maintains fixed input weights while the student's weights should be adapted over the course of learning such that it's membrane potential follows the

teacher's (Fig. 4B, C). The fitness  $\mathcal{F}(f)$  of an individual encoding the function  $f$  is measured by the root mean-squared error between the teacher and student membrane potential over the simulation duration  $T$ , excluding the initial 10%, averaged over  $n_{\text{exp}}$  experiments:

$$\mathcal{F}(f) := \frac{1}{n_{\text{exp}}} \sum_{k=1}^{n_{\text{exp}}} \sqrt{\sum_{t=0.1T}^T [v_k(t) - u_k(t)]^2}. \quad (5)$$

Each experiment consists of different input spike trains and different teacher weights. The general form of the plasticity rule for this error-driven learning task is given by:

$$\Delta w_j = \eta f(v, u, \bar{s}_j). \quad (6)$$

Using CGP with three inputs  $(v, u, \bar{s}_j)$ , we search for plasticity rules that maximize the fitness  $\mathcal{F}(f)$ .

Starting from low fitness, about half of the evolutionary runs evolve efficient plasticity rules (Fig. 4D) closely matching the performance of the stochastic gradient descent rule of [Urbanczik and Senn \(2014\)](#). While two runs evolve exactly Eq. 4, other solutions with comparable fitness are discovered, such as

$$\Delta w_j = \eta(v - u)\bar{s}_j \frac{(2u - 1)}{v}, \text{ and} \quad (7)$$

$$\Delta w_j = \eta\bar{s}_j(v + u) \frac{(v(v - u) - \bar{s}_j)}{v^2}. \quad (8)$$

At first sight, these rules may appear more complex, but for the considered parameter regime under the assumptions  $v \approx u; v, u \ll 1$ , we can write them as:

$$\Delta w_j = \eta c_1(v - u)\bar{s}_j + c_2, \quad (9)$$

with a multiplicative constant  $c_1 = \mathcal{O}(1)$  and a negligible additive constant  $c_2$ . Elementary manipulations of the expressions found by CGP thus demonstrate the similarity of these superficially different rules to Eq. 4. Consequently, they can be interpreted as approximations of the gradient-descent plasticity rule. The constants generally fall into two categories: fine-tuning of the learning rate for the set of task samples encountered during evolution ( $c_1$ ) and factors that have negligible influence and would most likely be pruned over longer evolutionary timescales ( $c_2$ ). This pruning could be accelerated, for example, by imposing a penalty on the model complexity in the fitness function, thus preferentially selecting simpler solutions.

In conclusion, the evolutionary search rediscovers variations of a human-designed efficient gradient-descent-based learning rule for the considered error-driven learning task. Due to the compact, interpretable representation of the plasticity rules we are able to analyze the set of high-performing solutions and thereby identify phenomenologically identical rules despite their superficial differences.

## 2.4 Evolving an efficient correlation-driven plasticity rule

We now consider a task in which neurons do not receive any feedback from the environment about their performance but instead only have access to correlations between pre- and postsynaptic activity. For this paradigm [Masquelier \(2017\)](#) proposes a correlation-driven plasticity rule that allows neurons to discover a repeating frozen-noise pattern interrupted by random background spikes. Their experimental setup is briefly described as follows:  $N$  inputs project to a single output neuron (Fig. 5A). The activity of all inputs is determined by a Poisson process with a fixed rate. A frozen-noise activity pattern of duration  $T_{\text{pattern}}$  is generated once and replayed every  $T_{\text{inter}}$  ms (Fig. 5B) while inputs are randomly spiking in between.

We define the fitness  $\mathcal{F}(f)$  of an individual encoding the function  $f$  by the minimal average signal-to-noise ratio SNR across  $n_{\text{exp}}$  experiments:

$$\mathcal{F}(f) := \min_k \{\text{SNR}_k, k \in [1, n_{\text{exp}}]\}. \quad (10)$$

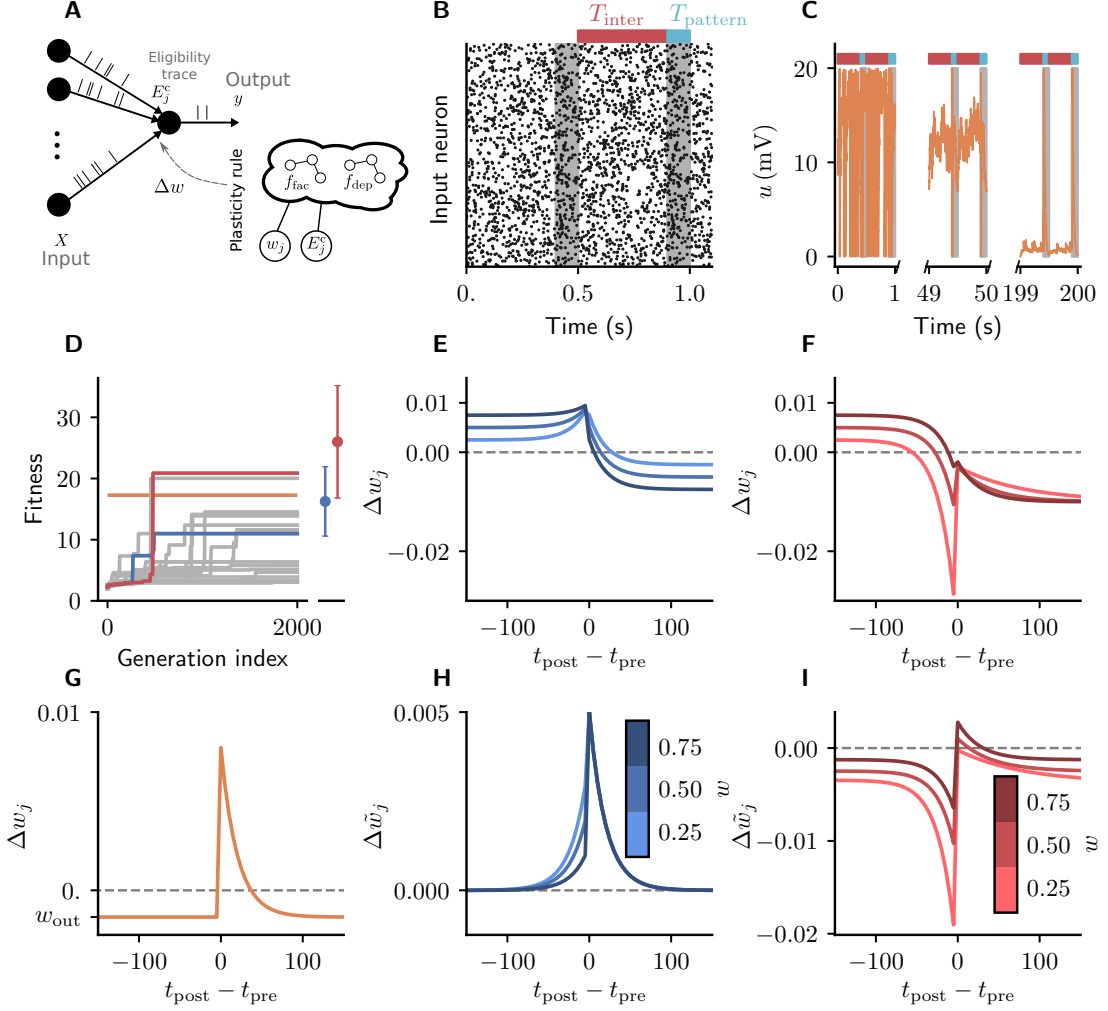


**Figure 5: Cartesian genetic programming evolves diverse correlation-driven learning rules.** (A) Network sketch. Multiple inputs project to a single output neuron. The current synaptic weight  $w_j$  and the eligibility trace  $E_j^c$  are provided to the plasticity rule that determines the weight update. (B) Activity of input units. A frozen-noise pattern of duration  $T_{\text{pattern}}$  (gray background) is interleaved with periods of random background spiking of duration  $T_{\text{inter}}$ . Spike trains are generated by a stationary Poisson process. (C) Membrane potential  $u$  of the output neuron over the course of learning using Eq. 12. Gray boxes indicate presentation of the frozen-noise pattern. (D) Fitness (Eq. 10) of the best individual per generation as a function of the generation index for multiple runs of the evolutionary algorithm with different initial conditions. Blue and red curves correspond to the two representative plasticity rules selected for detailed analysis. The orange line indicates the fitness of the homeostatic STDP rule (Eq. 12; [Masquelier, 2017](#)). Blue and red markers with error bars represent fitness of the two representative rules on 20 validation tasks not used during the evolutionary search. (E, F): Learning rules evolved by two runs of CGP (E: Eq. 14, F: Eq. 15): weight change  $\Delta w_j$  as a function of spike timing differences  $\Delta t_j$  for three different weights  $w_j$ . (G) Same for the homeostatic STDP rule (Eq. 12; [Masquelier, 2017](#)). (H, I) Effective learning rules: LR 1 (H, Eq. 17) and LR 2 (I, Eq. 18). The learning rate is  $\eta = 0.01$ .

The signal-to-noise ratio  $\text{SNR}_k$ , following [Masquelier \(2017\)](#), is defined as the difference between the maximal free membrane potential during pattern presentation averaged over multiple presentations ( $\langle u_{k,i,\text{max}} \rangle$ ) and the mean of the free membrane potential in between pattern presentations ( $\langle u_{k,\text{inter}} \rangle$ ) divided by its variance ( $\text{Var}(v_{k,\text{inter}})$ ):

$$\text{SNR}_k := \frac{\langle u_{k,i,\text{max}} \rangle - \langle u_{k,\text{inter}} \rangle}{\text{Var}(u_{k,\text{inter}})} . \quad (11)$$

The free membrane potential is obtained in a separate simulation with frozen weights by disabling the spiking mechanism for the output neuron. This removes measurement noise in the signal-to-noise ratio arising from spiking and subsequent membrane-potential reset. Each experiment consists of different realizations of a frozen-noise pattern and background spiking.

The rule described by [Masquelier \(2017\)](#) is a simple additive spike-timing-dependent plasticity (STDP) rule that replaces the depression branch of traditional STDP variants with a homeostatic term  $w_{\text{hom}} < 0$  ([Kempter et al., 1999](#)). The synaptic weight of the projection from input  $j$  changes at each postsynaptic spike according to (Fig. 5G):

$$\Delta w_j = \eta \begin{cases} w_{\text{hom}} & \Delta t_j < 0 \text{ (anticausal interaction)} \\ E_j^c + w_{\text{hom}} & \Delta t_j \geq 0 \text{ (causal interaction)} . \end{cases} \quad (12)$$

Here,  $E_j^c := e^{-|\Delta t_j|/\tau}$  represents an eligibility trace that depends on the relative timing of post- and presynaptic spiking ( $\Delta t_j = t_{\text{post}} - t_{\text{pre},j}$ ) and is represented locally in each synapse (e.g., [Morrison et al., 2008](#)).  $\eta$  represents a fixed learning rate and  $w_{\text{hom}}$  a constant. The synaptic weight is bound such that  $w_j \in [0, 1]$ . To illustrate the result of synaptic plasticity following Eq. 12, we consider the evolution of the membrane potential of an output neuron over the course of learning (Fig. 5C). While the target neuron spikes randomly at the beginning of learning, its membrane potential finally stays subthreshold in between pattern presentations and crosses threshold reliably upon pattern presentation.

We evolve learning rules of the following general form, which includes a dependence on the current synaptic weight in line with previously suggested STDP rules ([Gütig et al., 2003](#)) and subsumes Eq. 12 as a special case:

$$\Delta w_j = \eta \begin{cases} f_{\text{dep}}(w_j, E_j^c) & \Delta t_j < 0 \\ f_{\text{fac}}(w_j, E_j^c) & \Delta t_j \geq 0 . \end{cases} \quad (13)$$

Using CGP with two inputs  $(w_j, E_j^c)$ , we search for functions  $f_{\text{dep}}$  and  $f_{\text{fac}}$  that maximize the fitness  $\mathcal{F}(f_{\text{dep}}, f_{\text{fac}})$  (Eq. 10).

After 2000 generations, half of the runs of the evolutionary algorithm discover high-fitness solutions (Fig. 5D). These plasticity rules lead to synaptic weight configurations for which the signal-to-noise ratio of the free membrane potential is at least ten. Empirical investigation shows that such a signal-to-noise ratio, causes the neuron to reliably detect the frozen-noise pattern. From these well-performing learning rules, we pick two representative examples (Fig. 5E,F) to analyze in detail. Learning rule 1 (LR1, Fig. 5E) is defined by the following equation:

$$\Delta w_j = \eta \begin{cases} w_j - (w_j - 1)E_j^c & \Delta t_j < 0 \\ E_j^c - w_j & \Delta t_j \geq 0 . \end{cases} \quad (14)$$

Learning rule 2 (LR2, Fig. 5F) is defined by the following equation:

$$\Delta w_j = \eta \begin{cases} w_j - E_j^c/w_j & \Delta t_j < 0 \\ (w_j E_j^c)^{w_j} - 1 & \Delta t_j \geq 0 . \end{cases} \quad (15)$$

The direct availability of these rules as closed-form expressions enables an interesting line of inquiry. While both rules reliably enable the neuron to solve its task, they both exhibit nonzero facilitation and depression even for large time lags  $\Delta t_j$ , which immediately raises questions about their stability. To address this issue, we consider, for simplicity, a nearest-neighbor spike-pairing

scheme (e.g., Morrison et al., 2008) in which each postsynaptic spike can almost always be assigned a causal interaction with the preceding presynaptic spike and an anticausal interaction with the trailing presynaptic spike. Weight changes therefore come in pairs: for each causal update there must exist an anticausal one and vice-versa. In the limit of small firing rates, we can therefore make the simplifying assumption that each causal (anticausal) spike interaction is accompanied by an anticausal (causal) interaction with a large time difference  $\Delta t_j$  (see Appendix Sec. A for a mathematical argument). We can therefore construct effective learning rules by adding the asymptotic weight change for anticausal (causal) interactions to all weight changes on the causal (anticausal) branch:

$$\Delta \tilde{w}_j \rightarrow \frac{\eta}{2} \begin{cases} \Delta w_j(\Delta t_j) + \lim_{\Delta t'_j \rightarrow -\infty} \Delta w_j(\Delta t'_j) & \Delta t_j < 0 \\ \Delta w_j(\Delta t_j) + \lim_{\Delta t'_j \rightarrow \infty} \Delta w_j(\Delta t'_j) & \Delta t_j \geq 0 \end{cases} \quad (16)$$

We introduce the factor 1/2 to account for the fact that for the effective rules, in a nearest-neighbor spike-pairing scheme, each presynaptic spike is considered in two weight updates, once trailing, once preceding the postsynaptic spike. The disappearance of the long-term facilitating tails in the effective rules (Fig. 5H, I) confirms the stability of both learning rules, as previously reflected by their high fitness in simulations (Fig. 5D).

The form of the resulting effective learning rules suggests that they use distinct strategies to detect the repeated pattern. The effective LR1 (Fig. 5H)

$$\Delta \tilde{w}_j = \frac{\eta}{2} \begin{cases} (1 - w_j) E_j^c & \Delta t_j < 0 \\ E_j^c & \Delta t_j \geq 0 \end{cases} \quad (17)$$

decays to zero for large negative and positive time differences and causes facilitation for small time differences, regardless whether they are causal or anticausal. This learning rule favors correlation between presynaptic and postsynaptic firing with a small weight-dependent facilitation bias towards causal interactions. In contrast, effective LR2 (Fig. 5I)

$$\Delta w_j = \frac{\eta}{2} \begin{cases} -E_j^c/w_j + w_j - 1 & \Delta t_j < 0 \\ (w_j E_j^c)^{w_j} + w_j - 1 & \Delta t_j \geq 0 \end{cases} \quad (18)$$

implements a similar strategy as the learning rule of Masquelier (2017): it depresses the synapse for almost all interactions except for a narrow time window for small, positive (causal) time differences. Additionally, however, it more pronouncedly punishes anticausal interactions, thus being able to achieve even higher fitness. Note how both rules reproduce important components of experimentally established STDP traces (e.g., Caporale and Dan, 2008).

In conclusion, for the correlation-driven task, the evolutionary search is able to discover not only rules similar to those previously suggested but additionally proposes rules that are markedly different, yet still perform competitively, thus generating new hypotheses for learning in biological substrates. We note, again, that our insight into the dynamics of these rules was permitted, in the first place, by their interpretable representation in our evolutionary framework.

### 3 Discussion

Uncovering the mechanisms of learning via synaptic plasticity is a critical step towards understanding brain (dys)function and building truly intelligent, adaptive machines. We introduce a novel approach to discover biophysically plausible plasticity rules in spiking neuronal networks. Our meta-learning framework uses genetic programming to search for plasticity rules by optimizing a fitness function specific to the respective task family. Our approach discovers high-performing solutions in various learning paradigms, reward-driven, error-driven, and correlation-driven learning. This is, to the best of our knowledge, the first demonstration of the power of genetic programming methods in the search for plasticity mechanisms in spiking neuronal networks.

A key point of our approach is the compact representation of the plasticity rules. We restrict the complexity of the expressions by three considerations. First, we assume that effective descriptions

of weight changes can be found that are not unique to each individual synapse. This is a common assumption in computational neuroscience and based on the observation that nature must have found a parsimonious encoding of brain structure, as not every connection in the brain can be specified in the DNA of the organism (Zador, 2019); rather, genes encode general principles by which the neuronal networks and subnetworks are organized and reorganized (cf. Risi and Stanley, 2010). Our approach aims at discovering such general principles for synaptic plasticity. Second, physical considerations restrict the information available to the plasticity rule to local quantities, such as pre- and post-synaptic activity traces or specific signals delivered via neuromodulators (e.g., Miconi et al., 2018; Cox and Witten, 2019). Third, we limit the maximal size of the expressions to keep the resulting learning rules interpretable and avoid overfitting. We explicitly want to avoid constructing an opaque system that has high task performance but does not allow us to understand how the network structure is shaped over the course of learning. The low complexity of the resulting expressions generates intuitive understanding, facilitating communication and human-guided generalization from a set of solutions to different network architectures or task domains. In the search for plasticity rules suitable for physical implementations in biological systems, these insights are crucial as the identified plasticity mechanisms can serve as building blocks for learning rules that generalize to the actual challenges faced by biological agents. Moreover, simple expressions highlight the key interactions between the local variables giving rise to plasticity, thus providing insights into the underlying biophysical processes and potentially suggesting new experimental approaches.

Furthermore, the automated search can discover plasticity rules for a given problem that exploit implicit assumptions in the task. It therefore highlights underconstrained searches, be this due to scarcity of biological data, the simplicity of chosen tasks or the omission of critical features in the task design. For instance, without asserting equal average spike rates of background and pattern neurons in the correlation-driven task, one could discover plasticity rules that exploit the rate difference rather than the spatio-temporal structure of the input.

Future work needs to address a general issue of any optimization method: how can we systematically counter overfitting to reveal general solutions? A simple approach would increase the number of sample tasks during a single fitness evaluation. However, computational costs increase linearly in the number of samples. Another technique penalizes the complexity of the resulting expressions, e.g., proportional to the size of the computational graph. Since it is a priori unclear how this complexity penalty should be weighted against the original fitness measures, one should consider multi-objective optimization algorithms (e.g., Deb, 2001). Another issue to be addressed in future work is the choice of the learning rate. Currently, this value is not part of the optimization process and all tasks assume a fixed learning rate. One possibility is to allow for more constants in CGP such that the search can easily scale the learning rate. However, the dimensionality of the search space scales exponentially in the number of operators and constants, and the feasibility of such an approach needs to be carefully evaluated. One possibility to mitigate this combinatorial explosion is to combine the evolutionary search with gradient-based optimization methods that can fine-tune constants in the expressions (Topchy and Punch, 2001; Izzo et al., 2017).

Evolved Plastic Artificial Neural Networks (EPANNS; e.g., Soltoggio et al., 2018) and in particular adaptive HyperNEAT (Risi and Stanley, 2010), represent an alternative approach to designing plastic neural networks. In contrast to our method, however, these approaches include the network architecture itself into the evolutionary search, alongside synaptic plasticity rules. While this can lead to high-performance solutions due to a synergy between network architecture and plasticity, this interplay has an important drawback, as in general it is difficult to tease apart the contribution of plasticity from that of network structure to high task performance (cf. Gaier and Ha, 2019). In addition, the distributed, implicit representation of plasticity rules in HyperNEAT can be difficult to interpret, which hinders a deeper understanding of the learning mechanisms. In machine-learning-oriented applications, this lack of credit assignment is less of an issue. For research into plasticity rules employed by biological systems, however, it presents a significant obstacle.

The evolutionary search for plasticity rules requires a large number of simulations, as each candidate solution needs to be evaluated on a sufficiently large number of samples from the task family to encourage generalization (e.g., Chalmers, 1991; Bengio et al., 1992). Due to silent mutations in CGP, i.e., modifications of the genotype that do not alter the phenotype, we use caching methods to significantly reduce computational cost as only new solutions need to be

evaluated. However, even employing such methods, the number of required simulations remains large, in the order of  $10^3 - 10^4$  per evolutionary run. Neuromorphic systems, dedicated hardware specifically designed to emulate neuronal networks, provide an attractive way to speed up the evolutionary search. To serve as suitable substrates for the approach presented here, these systems should be able to emulate spiking neuronal networks in an accelerated fashion with respect to real time and provide on-chip plasticity with a flexible specification of plasticity mechanisms (e.g., [Davies et al., 2018](#); [Billaudelle et al., 2019](#); [Mayr et al., 2019](#)).

While the learning rules found in the experiments described above were all evolved from random expressions, one can also view the presented framework as a hypothesis-testing machine. Starting from a known plasticity rule, our framework would allow researchers to address questions like: assuming the learning rule would additionally have access to variable  $x$ , could this be incorporated into the weight updates such that learning would improve? The automated procedure makes answering such questions much more efficient than a human-guided manual search. Additionally, the framework is suitable to find robust biophysically plausible approximations for complex learning rules containing quantities that might be non-local, difficult to compute, and/or hard to implement in physical substrates. In particular, multi-objective optimization is suitable to evolve a known, complex rule into simpler versions while maintaining high task performance. Similarly, one could search for modifications of general rules that are purposefully tuned to quickly learn within a specific task family, outperforming more general solutions. In each of these cases, prior knowledge about effective learning algorithms provides a starting point from which the evolutionary search can discover powerful extensions.

The experiments considered here were mainly chosen due to their simplicity and prior knowledge about corresponding plasticity rules that provided us with a high-performance reference for comparison. Additionally, in each experiment, we have restricted ourselves to a constrained set of possible inputs to the plasticity rule. Future work may involve less preprocessed data as inputs while considering more diverse mathematical operators. In the correlation-driven task, one could for example provide the raw times of pre- and postsynaptic spiking to the graph instead of the exponential of their difference, leaving more freedom for the evolutionary search to discover creative solutions. We expect particularly interesting applications of our framework to involve more complex tasks that are challenging for contemporary algorithms, such as life-long learning, which needs to tackle the issue of catastrophic forgetting ([French, 1999](#)) or learning in recurrent spiking neuronal networks. In order to yield insights into information processing in the nervous system, the design of the network architecture should be guided by known anatomical features, while the considered task families should fall within the realm of ecologically relevant problems.

We view the presented methods as a machinery for generating, testing, and extending hypotheses on learning in spiking neuronal networks driven by problem instances and prior knowledge and constrained by experimental evidence. We believe this approach holds significant potential to accelerate progress towards deep insights into information processing in physical systems, both biological and biologically inspired, with immanent potential for the development of powerful artificial learning machines.

## 4 Materials and methods

### 4.1 Evolutionary algorithm

We use a  $\mu + \lambda$  evolution strategy ([Beyer and Schwefel, 2002](#)) to evolve a population of individuals towards high fitness. In each generation,  $\lambda$  new offsprings are created from  $\mu$  parents via tournament selection (e.g., [Miller et al., 1995](#)) and subsequent mutation. From these  $\mu + \lambda$  individuals the best  $\mu$  individuals are selected as parents for the next generation (Alg. 1). In this work we use a tournament size of one and a fixed mutation probability  $p_{\text{mutate}}$  for each gene in an offspring individual. Since in CGP crossover of individuals can lead to significant disruption of the search process due to major changes in the computational graphs ([Miller, 1999](#)), we avoid it here, in other words, new offspring are only modified by mutations. We use neutral search ([Miller and Thomson, 2000](#)), in which an offspring is preferred over a parent with equal fitness, to allow the accumulation of silent mutations that can jointly lead to an increase in fitness. As it is computationally infeasible to exhaustively evaluate an individual on all possible tasks from a task family, we evaluate individuals

```

Data: Initial random parent Population  $P_0 = \{p_i\}$  of size  $\mu$ 
 $t \leftarrow 0$ 
while  $t < n_{\text{generations}}$  do
| Create new offspring population  $Q_t = \text{CreateOffspringPopulation}(P_t)$ 
| Combine parent + offspring populations  $R_t = P_t \cup Q_t$ 
| Evaluate fitness of each individual in  $R_t$ 
| Pick  $P_{t+1} \subset R_t$  best individuals as new parents
|  $t \leftarrow t + 1$ 
end
Function  $\text{CreateOffspringPopulation}(P)$ 
begin
| Offspring population  $Q = \{\}$ 
| while  $|Q| < \lambda$  do
| | Choose random subset of  $P$  of size  $N_{\text{tournament}}$ 
| | Choose best individual in the subset and append to  $Q$ 
| end
| for  $q_i \in Q$  do
| | Mutate each gene of  $q_i$  with mutation probability  $p_{\text{mutation}}$ 
| end
| Return  $Q$ 
end

```

**Algorithm 1:** Variant of  $\mu + \lambda$  evolution strategies used in this study. Note the absence of a crossover step.

only on a limited number of sample tasks and aggregate the results into a scalar fitness, either by choosing the minimal result or averaging. We manually select the number of sample tasks to balance computational costs and sampling noise for each task. In each generation, we use the same initial conditions to allow a meaningful comparison of results across generations. If an expression is encountered that can not be meaningfully evaluated, such as division by zero, the corresponding individual is assigned a fitness of  $-\infty$ .

## 4.2 HAL-CGP

HAL-CGP (<https://github.com/Happy-Algorithms-League/hal-cgp>) is an extensible pure Python library implementing Cartesian genetic programming to represent, mutate and evaluate populations of individuals encoding symbolic expressions targeting applications with computationally expensive fitness evaluations. It supports the translation from a CGP genotype, a two-dimensional Cartesian graph, into the corresponding phenotype, a computational graph implementing a particular mathematical expression. These computational graphs can be exported as pure Python functions, NumPy-compatible functions (Walt et al., 2011), SymPy expressions (Meurer et al., 2017) or PyTorch modules (Paszke et al., 2017). Users define the structure of the two-dimensional graph from which the computational graph is generated. This includes the number of inputs, columns, rows, and outputs, as well as the computational primitives, i.e., mathematical operators and constants, that compose the mathematical expressions. Due to the modular design of the library, users can easily implement new operators to be used as primitives. The library implements a  $\mu + \lambda$  evolution strategy to evolve individuals (see Sec. 4.1). Users need to specify hyperparameters for the evolutionary algorithm, such as the size of parent and offspring populations and the maximal number of generations. To avoid reevaluating phenotypes that have been previously evaluated, the library provides a mechanism for caching results on disk. Exploiting the wide availability of multi-core architectures, the library can parallelize the evaluation of all individuals in a single generation via separate processes.

## 4.3 NEST simulator

Spiking neuronal network simulations are based on the 2.16.0 release of the NEST simulator (Gewaltig and Diesmann, 2007) (<https://github.com/nest/nest-simulator>; commit 3c6f0f3). NEST

is an open-source simulator for spiking neuronal networks with a focus on large networks with simple neuron models. The computationally intensive propagation of network dynamics is implemented in C++ while the network model can be specified using a Python API (PyNEST; [Eppler et al., 2009](#); [Zaytsev and Morrison, 2014](#)). NEST profits from modern multi-core and multi-node systems by combining local parallelization with OpenMP threads and inter-node communication via the Message Passing Interface (MPI) ([Jordan et al., 2018](#)). The standard distribution offers a variety of established neuron and plastic synapse models, including variants of spike-timing-dependent plasticity, reward-modulated plasticity and structural plasticity. New models can be implemented via a domain-specific language ([Plotnikov et al., 2016](#)) or custom C++ code. For the purpose of this study, we implemented a reward-driven (Eq. 2; [Urbanczik and Senn, 2009](#)) and an error-driven learning rule (Eq. 4; [Urbanczik and Senn, 2014](#)), as well as a homeostatic STDP rule (Eq. 12; [Masquelier, 2017](#)) via custom C++ code. Due to the specific implementation of spike delivery in NEST, we introduce a constant in the STDP rule that is added at each facilitation call instead of using a separate depression term. To support arbitrary mathematical expressions in the error-driven (Eq. 6) and correlation-driven synapse models (Eq. 13), we additionally implemented variants in which the weight update can be specified via SymPy compatible strings ([Meurer et al., 2017](#)) that are parsed by SymEngine (<https://github.com/symengine/symengine>), a C++ library for symbolic computation.

#### 4.4 Computing systems

All experiments were performed on JUWELS (Jülich Wizard for European Leadership Science), an HPC system at the Jülich Research Centre, Jülich, Germany, with 12 Petaflop peak performance. The system contains 2271 general-purpose compute nodes, each equipped with two Intel Xeon Platinum 8168 processors (2x24cores) and 12x8GB main memory. Compute nodes are connected via an EDR-Infiniband fat-tree network and run CentOS 7. Each experiment employed a single compute node.

#### 4.5 Reward-driven learning task

We consider a reinforcement learning task for spiking neurons similar to [Urbanczik and Senn \(2009\)](#). Spiking activity of the output neuron is generated by an inhomogeneous Poisson process with instantaneous rate  $\phi$  determined by its membrane potential  $u$  ([Pfister et al., 2006](#); [Urbanczik and Senn, 2009](#)):

$$\phi(u) := \rho e^{\frac{u-u_{\text{th}}}{\Delta u}}. \quad (19)$$

Here,  $\rho$  is the firing rate at threshold,  $u_{\text{th}}$  the threshold potential, and  $\Delta u$  a parameter governing the noise amplitude. In contrast to [Urbanczik and Senn \(2009\)](#), we consider an instantaneous reset of the membrane potential after a spike instead of an hyperpolarization kernel. The output neuron receives spike trains from sources randomly drawn from an input population of size  $N$  with randomly initialized weights ( $w_{\text{initial}} \sim \mathcal{N}(0, \sigma_w)$ ). Before each pattern presentation, the output neurons membrane potential and synaptic currents are reset. The eligibility trace in every synapse is updated in continuous time according to the following differential equation ([Urbanczik and Senn, 2009](#)):

$$\tau_M \dot{E}_j^r = -E_j^r + \frac{1}{\Delta u} \left[ \sum_{s \in y} \delta(t-s) - \phi(u(t)) \right] \bar{s}_j(t), \quad (20)$$

where  $\tau_M$  governs the time scale of the eligibility trace,  $\Delta u$  is a parameter of the postsynaptic cell governing its noise amplitude,  $y$  represents the postsynaptic spike train, and  $\bar{s}_j(t) = (\kappa * s_j)(t)$  the presynaptic spike train  $s_j$  filtered by the synaptic kernel  $\kappa$ . The learning rate  $\eta$  was manually tuned to obtain high performance with Eq. 2.

#### 4.6 Error-driven learning task

We consider an error-driven learning task for spiking neurons similar to [Urbanczik and Senn \(2014\)](#).  $N$  Poisson inputs with constant rates ( $r_i \sim \mathcal{U}[r_{\text{min}}, r_{\text{max}}], i \in [1, N]$ ) project to a teacher neuron

and, with the same connectivity pattern, to a student neuron. Spiking activity of the output neuron is generated by an inhomogeneous Poisson process with instantaneous rate  $\phi$  determined by its membrane potential  $u$  (Pfister et al., 2006; Urbanczik and Senn, 2009):

$$\phi(u) := \rho e^{\frac{u-u_{\text{th}}}{\Delta u}}. \quad (21)$$

Here,  $\rho$  is the firing rate at threshold,  $u_{\text{th}}$  the threshold potential, and  $\Delta u$  a parameter governing the noise amplitude. In contrast to Sec. 4.5, the membrane potential is not reset after spike emission. Fixed synaptic weights from the inputs to the teacher are uniformly sampled from the interval  $[w_{\text{min}}, w_{\text{max}}]$ , while weights to the student are all initialized to a fixed value  $w_0$ . In each trial we randomly shift all teacher weights by a global value  $w_{\text{shift}}$  to avoid a bias in the error signal that may arise if the teacher membrane potential is initially always larger or always smaller than the student membrane potential. Target potentials are read out from the teacher every  $\delta t$  and provided instantaneously to the student. The learning rate  $\eta$  was chosen via grid search on a single example task for high performance with Eq. 4.

## 4.7 Correlation-driven learning task

We consider an correlation-driven learning task for spiking neurons similar to Masquelier (2017): a spiking neuron, modeled as a leaky integrate-and-fire neuron with delta-shaped post-synaptic currents, receives stochastic spike trains from  $N$  inputs via plastic synapses.

To construct the input spike trains, we first create a frozen-noise pattern by drawing random spikes  $S_i^{\text{pattern}} \in [0, T_{\text{pattern}}]$ ,  $i \in [0, N - 1]$  from a Poisson process with rate  $\nu$ . Neurons that fire at least once in this pattern are in the following called “pattern neurons”, the remaining are called “background neurons”. We alternate this frozen-noise pattern with random spike trains of length  $T_{\text{inter}}$  generated by a Poisson process with rate  $\nu$  (Fig. 5B). To balance the average rates of pattern neurons and background neurons, we reduce the spike rate of pattern neurons in between patterns by a factor  $\alpha$ . Background neurons have an average rate of  $\nu_{\text{inter}} = \nu \frac{T_{\text{inter}}}{T_{\text{inter}} + T_{\text{pattern}}}$ . We assume that pattern neurons spike only once during the pattern. Thus, they have an average rate of  $\nu = \alpha \nu_{\text{inter}} + \frac{1}{T_{\text{inter}} + T_{\text{pattern}}} = \alpha \nu_{\text{inter}} + \nu_{\text{pattern}}$ . Plugging in the previous expression for  $\nu_{\text{inter}}$  and solving for  $\alpha$  yields  $\alpha = 1 - \frac{\nu_{\text{pattern}}}{\nu_{\text{inter}}}$ . We choose the same learning rate as Masquelier (2017).

## 5 Acknowledgments

We gratefully acknowledge funding from the European Union, under grant agreements 604102, 720270, 785907 (HBP) and the Manfred Stärk Foundation. We further express our gratitude towards the Gauss Centre for Supercomputing e.V. ([www.gauss-centre.eu](http://www.gauss-centre.eu)) for co-funding this project by providing computing time through the John von Neumann Institute for Computing (NIC) on the GCS Supercomputer JUWELS at Jülich Supercomputing Centre (JSC). We would like to thank all participants from the HBP SP9 Fürberg meetings for stimulating interactions and Tomoki Fukai for initial discussions and support. We also thank Henrik Mettler for helpful comments on the manuscript. All network simulations carried out with NEST ([www.nest-simulator.org](http://www.nest-simulator.org)).

## 6 Competing interests

The authors declare no competing interests.

## References

Andrychowicz, M., Denil, M., Gomez, S., Hoffman, M. W., Pfau, D., Schaul, T., and de Freitas, N. (2016). Learning to learn by gradient descent by gradient descent. In *Advances in Neural Information Processing Systems*, pages 3981–3989.

Artola, A., Brocher, S., and Singer, W. (1990). Different voltage-dependent thresholds for inducing long-term depression and long-term potentiation in slices of rat visual cortex. *Nature*, 347(6288):69.

Bengio, S., Bengio, Y., and Cloutier, J. (1994). Use of genetic programming for the search of a new learning rule for neural networks. In *Evolutionary Computation, 1994. IEEE World Congress on Computational Intelligence., Proceedings of the First IEEE Conference on*, pages 324–327. IEEE.

Bengio, S., Bengio, Y., Cloutier, J., and Gecsei, J. (1992). On the optimization of a synaptic learning rule. In *Preprints Conf. Optimality in Artificial and Biological Neural Networks*, pages 6–8. Univ. of Texas.

Bengio, S., Bengio, Y., Cloutier, J., and Gecsei, J. (1993). Generalization of a parametric learning rule. In *ICANN93*, pages 502–502. Springer.

Bengio, Y., Bengio, S., and Cloutier, J. (1990). *Learning a synaptic learning rule*. Université de Montréal, Département d'informatique et de recherche opérationnelle.

Beyer, H.-G. and Schwefel, H.-P. (2002). Evolution strategies—a comprehensive introduction. *Natural computing*, 1(1):3–52.

Bi, G.-q. and Poo, M.-m. (1998). Synaptic modifications in cultured hippocampal neurons: dependence on spike timing, synaptic strength, and postsynaptic cell type. *J. Neurosci.*, 18(24):10464–10472.

Billaudelle, S., Stradmann, Y., Schreiber, K., Cramer, B., Baumbach, A., Dold, D., Göltz, J., Kungl, A. F., Wunderlich, T. C., Hartel, A., et al. (2019). Versatile emulation of spiking neural networks on an accelerated neuromorphic substrate. *arXiv preprint arXiv:1912.12980*.

Bohnstingl, T., Scherr, F., Pehle, C., Meier, K., and Maass, W. (2019). Neuromorphic hardware learns to learn. *Frontiers in neuroscience*, 13.

Caporale, N. and Dan, Y. (2008). Spike timing-dependent plasticity: a hebbian learning rule. *Annu. Rev. Neurosci.*, 31:25–46.

Chalmers, D. J. (1991). The evolution of learning: An experiment in genetic connectionism. In *Connectionist Models*, pages 81–90. Elsevier.

Clopath, C., Büsing, L., Vasilaki, E., and Gerstner, W. (2010). Connectivity reflects coding: a model of voltage-based stdp with homeostasis. *Nat. Neurosci.*, 13(3):344.

Cox, J. and Witten, I. B. (2019). Striatal circuits for reward learning and decision-making. *Nature Reviews Neuroscience*, page 1.

Davies, M., Srinivasa, N., Lin, T.-H., Chinya, G., Cao, Y., Choday, S. H., Dimou, G., Joshi, P., Imam, N., Jain, S., et al. (2018). Loihi: A neuromorphic manycore processor with on-chip learning. *IEEE Micro*, 38(1):82–99.

Deb, K. (2001). *Multi-objective optimization using evolutionary algorithms*, volume 16. John Wiley & Sons.

Deneve, S. (2008). Bayesian spiking neurons i: inference. *Neural computation*, 20(1):91–117.

Dold, D., Bytschok, I., Kungl, A. F., Baumbach, A., Breitwieser, O., Senn, W., Schemmel, J., Meier, K., and Petrovici, M. A. (2019). Stochasticity from functionwhy the bayesian brain may need no noise. *Neural networks*, 119:200–213.

Dudek, S. M. and Bear, M. F. (1993). Bidirectional long-term modification of synaptic effectiveness in the adult and immature hippocampus. *J. Neurosci.*, 13(7):2910–2918.

Eppler, J. M., Helias, M., Muller, E., Diesmann, M., and Gewaltig, M.-O. (2009). PyNEST: a convenient interface to the NEST simulator. *Frontiers in neuroinformatics*, 2:12.

French, R. M. (1999). Catastrophic forgetting in connectionist networks. *Trends in cognitive sciences*, 3(4):128–135.

Gaier, A. and Ha, D. (2019). Weight agnostic neural networks. *arXiv preprint arXiv:1906.04358*.

Gewaltig, M.-O. and Diesmann, M. (2007). NEST (Neural Simulation Tool). *Scholarpedia*, 2(4):1430.

Göltz, J., Baumbach, A., Billaudelle, S., Breitwieser, O., Dold, D., Kriener, L., Kungl, A. F., Senn, W., Schemmel, J., Meier, K., et al. (2019). Fast and deep neuromorphic learning with time-to-first-spike coding. *arXiv preprint arXiv:1912.11443*.

Goodfellow, I., Bengio, Y., and Courville, A. (2016). *Deep learning*. MIT press.

Gütig, R., Aharonov, R., Rotter, S., and Sompolinsky, H. (2003). Learning input correlations through nonlinear temporally asymmetric hebbian plasticity. *J. Neurosci.*, 23(9):3697–3714.

Ivakhnenko, A. G. (1971). Polynomial theory of complex systems. *IEEE transactions on Systems, Man, and Cybernetics*, (4):364–378.

Izhikevich, E. M. (2007). Solving the distal reward problem through linkage of stdp and dopamine signaling. *Cereb. Cortex*, 17(10):2443–2452.

Izzo, D., Biscani, F., and Mereta, A. (2017). Differentiable genetic programming. In *European Conference on Genetic Programming*, pages 35–51. Springer.

Jordan, J., Ippen, T., Helias, M., Kitayama, I., Sato, M., Igarashi, J., Diesmann, M., and Kunkel, S. (2018). Extremely scalable spiking neuronal network simulation code: from laptops to exascale computers. *Frontiers in neuroinformatics*, 12:2.

Jordan, J., Petrovici, M. A., Breitwieser, O., Schemmel, J., Meier, K., Diesmann, M., and Tetzlaff, T. (2019). Deterministic networks for probabilistic computing. *Scientific reports*, 9(1):1–17.

Kappel, D., Habenschuss, S., Legenstein, R., and Maass, W. (2015). Network plasticity as bayesian inference. *PLoS Comput. Biol.*, 11(11):e1004485.

Kempter, R., Gerstner, W., and van Hemmen, J. L. (1999). Hebbian learning and spiking neurons. *Phys. Rev. E*, 59:4498–4514.

Keup, C., Kühn, T., Dahmen, D., and Helias, M. (2020). Transient chaotic dimensionality expansion by recurrent networks. *arXiv preprint arXiv:2002.11006*.

Koza, J. R. (1992). *Genetic programming: on the programming of computers by means of natural selection*, volume 1. MIT press.

Koza, J. R. (2010). Human-competitive results produced by genetic programming. *Genetic Programming and Evolvable Machines*, 11(3-4):251–284.

Kutschireiter, A., Surace, S. C., Sprekeler, H., and Pfister, J.-P. (2017). Nonlinear bayesian filtering and learning: a neuronal dynamics for perception. *Scientific reports*, 7(1):8722.

Marblestone, A. H., Wayne, G., and Kording, K. P. (2016). Toward an integration of deep learning and neuroscience. *Frontiers in computational neuroscience*, 10:94.

Masquelier, T. (2017). STDP allows close-to-optimal spatiotemporal spike pattern detection by single coincidence detector neurons. *Neuroscience*, pages 1–8.

Mayr, C., Hoeppner, S., and Furber, S. (2019). Spinnaker 2: A 10 million core processor system for brain simulation and machine learning. *arXiv preprint arXiv:1911.02385*.

Meurer, A., Smith, C. P., Paprocki, M., Čertík, O., Kirpichev, S. B., Rocklin, M., Kumar, A., Ivanov, S., Moore, J. K., Singh, S., et al. (2017). Sympy: symbolic computing in python. *PeerJ Computer Science*, 3:e103.

Miconi, T., Rawal, A., Clune, J., and Stanley, K. O. (2018). Backpropamine: training self-modifying neural networks with differentiable neuromodulated plasticity.

Miller, B. L., Goldberg, D. E., et al. (1995). Genetic algorithms, tournament selection, and the effects of noise. *Complex systems*, 9(3):193–212.

Miller, J. and Thomson, P. (2000). Cartesian genetic programming. In *Proc. European Conference on Genetic Programming*, volume 1802, pages 121–132. Springer.

Miller, J. F. (1999). An empirical study of the efficiency of learning boolean functions using a cartesian genetic programming approach. In *Proceedings of the 1st Annual Conference on Genetic and Evolutionary Computation- Volume 2*, pages 1135–1142. Morgan Kaufmann Publishers Inc.

Miller, J. F. (2011). Cartesian genetic programming. In *Cartesian Genetic Programming*, pages 17–34. Springer.

Moradi, S., Qiao, N., Stefanini, F., and Indiveri, G. (2017). A scalable multicore architecture with heterogeneous memory structures for dynamic neuromorphic asynchronous processors (dynaps). *IEEE transactions on biomedical circuits and systems*, 12(1):106–122.

Morrison, A., Diesmann, M., and Gerstner, W. (2008). Phenomenological models of synaptic plasticity based on spike timing. *Biological cybernetics*, 98(6):459–478.

Ngezahayo, A., Schachner, M., and Artola, A. (2000). Synaptic activity modulates the induction of bidirectional synaptic changes in adult mouse hippocampus. *J. Neurosci.*, 20(7):2451–2458.

Nordlie, E., Gewaltig, M.-O., and Plesser, H. E. (2009). Towards reproducible descriptions of neuronal network models. *PLoS computational biology*, 5(8).

Orchard, J. and Wang, L. (2016). The evolution of a generalized neural learning rule. In *Neural Networks (IJCNN), 2016 International Joint Conference on*, pages 4688–4694. IEEE.

Paszke, A., Gross, S., Chintala, S., Chanan, G., Yang, E., DeVito, Z., Lin, Z., Desmaison, A., Antiga, L., and Lerer, A. (2017). Automatic differentiation in pytorch.

Pfister, J.-P., Dayan, P., and Lengyel, M. (2010). Synapses with short-term plasticity are optimal estimators of presynaptic membrane potentials. *Nature neuroscience*, 13(10):1271.

Pfister, J.-P., Toyoizumi, T., Barber, D., and Gerstner, W. (2006). Optimal spike-timing-dependent plasticity for precise action potential firing in supervised learning. *Neural computation*, 18(6):1318–1348.

Plotnikov, D., Rumpe, B., Blundell, I., Ippen, T., Eppler, J. M., and Morrison, A. (2016). NESTML: a modeling language for spiking neurons. *arXiv preprint arXiv:1606.02882*.

Radi, A. and Poli, R. (2003). Discovering efficient learning rules for feedforward neural networks using genetic programming. In *Recent advances in intelligent paradigms and applications*, pages 133–159. Springer.

Risi, S. and Stanley, K. O. (2010). Indirectly encoding neural plasticity as a pattern of local rules. In *International Conference on Simulation of Adaptive Behavior*, pages 533–543. Springer.

Rumelhart, D. E., Hinton, G. E., and Williams, R. J. (1985). Learning internal representations by error propagation. Technical report, California Univ San Diego La Jolla Inst for Cognitive Science.

Sacramento, J., Costa, R. P., Bengio, Y., and Senn, W. (2018). Dendritic cortical microcircuits approximate the backpropagation algorithm. In *Advances in Neural Information Processing Systems*, pages 8721–8732.

Soltoggio, A., Stanley, K. O., and Risi, S. (2018). Born to learn: the inspiration, progress, and future of evolved plastic artificial neural networks. *Neural Networks*.

Topchy, A. and Punch, W. F. (2001). Faster genetic programming based on local gradient search of numeric leaf values. In *Proceedings of the 3rd Annual Conference on Genetic and Evolutionary Computation*, pages 155–162. Morgan Kaufmann Publishers Inc.

Toyoizumi, T., Pfister, J.-P., Aihara, K., and Gerstner, W. (2005). Generalized bienenstock-cooper-munro rule for spiking neurons that maximizes information transmission. *Proceedings of the National Academy of Sciences of the United States of America*, 102(14):5239–5244.

Urbanczik, R. and Senn, W. (2009). Reinforcement learning in populations of spiking neurons. *Nature neuroscience*, 12(3):250.

Urbanczik, R. and Senn, W. (2014). Learning by the dendritic prediction of somatic spiking. *Neuron*, 81(3):521–528.

Walt, S. v. d., Colbert, S. C., and Varoquaux, G. (2011). The numpy array: a structure for efficient numerical computation. *Computing in Science & Engineering*, 13(2):22–30.

Whittington, J. C. and Bogacz, R. (2019). Theories of error back-propagation in the brain. *Trends in cognitive sciences*.

Zador, A. M. (2019). A critique of pure learning and what artificial neural networks can learn from animal brains. *Nature communications*, 10(1):1–7.

Zaytsev, Y. V. and Morrison, A. (2014). CyNEST: a maintainable cython-based interface for the NEST simulator. *Frontiers in neuroinformatics*, 8:23.

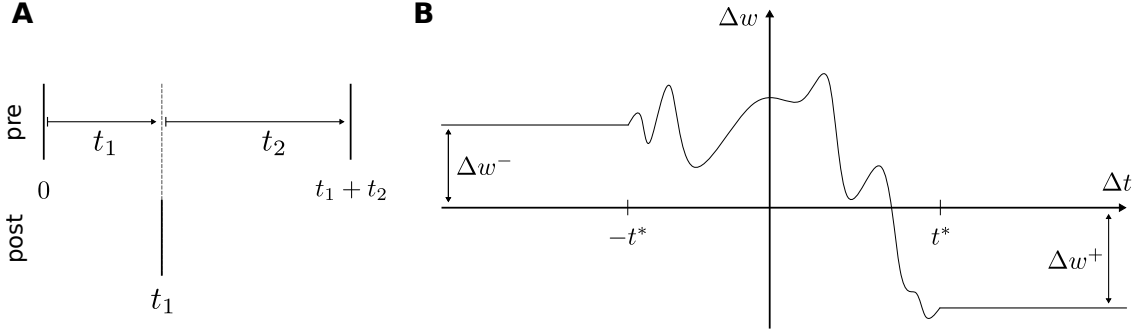


Figure 6: **Derivation of effective learning rules.** (A) A postsynaptic spike at  $t = t_1$  paired with a causal presynaptic spike at  $t = 0$  and anticausal presynaptic spike at  $t = t_1 + t_2$ . (B) The general form of the learning rules considered in the derivation of Eq. 22. The learning rule varies only on a restricted interval of time differences between  $-t^*$  and  $t^*$  where it is bounded from above and below, while it remains constant outside this interval.

## A Derivation of effective learning rules

We consider the effective weight change resulting from a pair of causal ( $t_{\text{post}} > t_{\text{pre}}$ ) and anticausal ( $t_{\text{post}} < t_{\text{pre}}$ ) spikes. Note that the approximation of considering only nearest-neighbor spikes becomes more accurate as the firing of pre- and postsynaptic neurons become more similar. Without loss of generality we assume a causal presynaptic spike at  $t = 0$  and a postsynaptic spike at  $t = t_1$  are accompanied by an anticausal presynaptic spike at  $t = t_1 + t_2$  with arbitrary  $t_2 \geq 0$  (Fig. 6A). Assuming presynaptic spikes are generated by a stationary Poisson process with rate  $\nu$ , the probability to observe the anticausal spike at  $t = t_1 + t_2$  is given by:  $p(t_1 + t_2 | t_1) = \nu e^{-\nu t_2}$ . We consider a plasticity rule  $\Delta w(\Delta t)$  which only depends on the time difference  $\Delta t$  of pre- and postsynaptic spikes. Additionally we assume that  $\Delta w(\Delta t)$  only varies within  $|\Delta t| < t^*$  and is constant outside these bounds (Fig. 6B). Note that this is an approximation to the learning rules described in the main text which are not constant outside specific bounds but rather decay exponentially over a characteristic time scale  $\tau$ . We account for considering each presynaptic spike in two weight updates, once preceding, once trailing the presynaptic spike, by introducing the factor 1/2. The resulting weight change from a causal and an anticausal spike can hence be written as:

$$\begin{aligned}
\Delta \tilde{w}(t_1) &= \frac{1}{2} \Delta w(t_1) + \frac{1}{2} \langle \Delta w(-t_2) \rangle_{p(t_1+t_2|t_1)} \\
&= \frac{1}{2} \Delta w(t_1) + \frac{1}{2} \int_0^\infty dt_2 p(t_1 + t_2 | t_1) \Delta w(-t_2) \\
&= \frac{1}{2} \Delta w(t_1) + \frac{1}{2} \underbrace{\int_0^{t^*} dt_2 \nu e^{-\nu t_2} \Delta w(-t_2)}_{\leq \Delta w_{\max} (-e^{-\nu t^*} + 1) \underset{\nu \ll \frac{1}{t^*}}{\approx} 0} + \frac{1}{2} \Delta w^- \underbrace{\int_{t^*}^\infty dt_2 \nu e^{-\nu t_2}}_{=(-0 + e^{-\nu t^*}) \underset{\nu \ll \frac{1}{t^*}}{\approx} 1} \\
&\geq \Delta w_{\min} (-e^{-\nu t^*} + 1) \underset{\nu \ll \frac{1}{t^*}}{\approx} 0 \\
&\approx \frac{1}{2} \Delta w(t_1) + \frac{1}{2} \Delta w^- \tag{22}
\end{aligned}$$

On line three we used the premise that  $\Delta w(t)$  is bounded from above and below by  $\Delta w_{\max}$  and  $\Delta w_{\min}$ , respectively. Additionally, we considered a regime in which presynaptic firing rates are small compared to the timescale on which  $\Delta w(t)$  varies significantly ( $\nu \ll \frac{1}{t^*}$ ). The characteristic time scale of learning rules in the main text is  $\tau = 20$  ms. With a presynaptic firing rate of 3 Hz this approximation holds in our experiments.

## B Simulation details

Table 1, Table 2, and Table 3 summarize the network models used in the experiments.

A Model summary		
<b>Populations</b>	2	
<b>Topology</b>	—	
<b>Connectivity</b>	Feedforward with fixed connection probability	
<b>Neuron model</b>	Leaky integrate-and-fire (LIF) with exponential post-synaptic currents	
<b>Plasticity</b>	Reward-driven	
<b>Measurements</b>	Spikes	
B Populations		
Name	Elements	Size
Input	Spike generators with pre-defined spike trains (see Sec. 4.5)	$N$
Output	LIF neuron	1
C Connectivity		
Source	Target	Pattern
Input	Output	Fixed pairwise connection probability $p$ ; synaptic delay $d$ ; random initial weights from $\mathcal{N}(0, \sigma_w^2)$
D Neuron model		
<b>Type</b>	LIF neuron with exponential post-synaptic currents	
<b>Subthreshold dynamics</b>	$\frac{du(t)}{dt} = -\frac{u(t) - E_L}{\tau_m} + \frac{I_s(t)}{C_m} \text{ if not refractory}$ $u(t) = u_r \text{ else}$	
<b>Spiking</b>	$I_s(t) = \sum_{i,k} w_k e^{-(t-t_i^k)/\tau_s} \Theta(t - t_i^k)$ , $k$ : neuron index, $i$ : spike index Stochastic spike generation via inhomogeneous Poisson process with intensity $\phi(u) = \rho e^{(u-u_{th})/\Delta u}$ ; reset of $u$ to $u_r$ after spike emission and refractory period of $\tau_r$	
E Synapse model		
<b>Plasticity</b>	Reward-driven with episodic update (Eq. 2, Eq. 3)	
<b>Other</b>	Each synapse stores an eligibility trace (Eq. 20)	
F Simulation Parameters		
<b>Populations</b>	$N = 50$	
<b>Connectivity</b>	$p = 0.8, \sigma_w = 10^3 \text{ pA}$	
<b>Neuron model</b>	$\rho = 0.01 \text{ Hz}, \Delta u = 0.2 \text{ mV}, E_L = -70 \text{ mV}, u_r = -70 \text{ mV}, u_{th} = -55 \text{ mV}, \tau_m = 10 \text{ ms}, C_m = 250 \text{ pF}, \tau_r = 2 \text{ ms}, \tau_s = 2 \text{ ms}$	
<b>Synapse model</b>	$\eta = 10, \tau_M = 500 \text{ ms}, d = 1 \text{ ms}$	
<b>Input</b>	$M = 30, r = 6 \text{ Hz}, T = 500 \text{ ms}, n_{\text{training}} = 500, n_{\text{exp}} = 10$	
<b>Other</b>	$h = 0.01 \text{ ms}$	
G CGP Parameters		
<b>Population</b>	$\mu = 4, p_{\text{mutation}} = 0.045$	
<b>Genome</b>	$n_{\text{inputs}} = 2, n_{\text{outputs}} = 1, n_{\text{rows}} = 1, n_{\text{columns}} = 5, l_{\text{max}} = 5$	
<b>Primitives</b>	Add, Sub, Mul, Div, Const(1.0)	
<b>EA</b>	$\lambda = 4, n_{\text{breeding}} = 4, n_{\text{tournament}} = 1$	
<b>Other</b>	max generations = 500, minimal fitness = 300	

Table 1: Description of the network model used in the reward-driven learning task (Sec. 4.5) (according to Nordlie et al., 2009).

A Model summary		
<b>Populations</b>	3	
<b>Topology</b>	—	
<b>Connectivity</b>	Feedforward with all-to-all connections	
<b>Neuron model</b>	Leaky integrate-and-fire (LIF) with exponential post-synaptic currents	
<b>Plasticity</b>	Error-driven	
<b>Measurements</b>	Spikes, membrane potentials	
B Populations		
Name	Elements	Size
Input	Spike generators with pre-defined spike trains (see Sec. 4.6)	$N$
Teacher	LIF neuron	1
Student	LIF neuron	1
C Connectivity		
Source	Target	Pattern
Input	Teacher	All-to-all; synaptic delay $d$ ; random weights $w \sim \mathcal{U}[w_{\min}, w_{\max}]$ ; weights randomly shifted by $w_{\text{shift}}$ on each trial
Input	Student	All-to-all; synaptic delay $d$ ; fixed initial weights $w_0$
D Neuron model		
<b>Type</b>	LIF neuron with exponential post-synaptic currents	
<b>Subthreshold dynamics</b>	$\frac{du(t)}{dt} = -\frac{u(t) - E_L}{\tau_m} + \frac{I_s(t)}{C_m}$ $I_s(t) = \sum_{i,k} J_k e^{-(t-t_i^k)/\tau_s} \Theta(t - t_i^k)$ $k$ : neuron index, $i$ : spike index	
<b>Spiking</b>	Stochastic spike generation via inhomogeneous Poisson process with intensity $\phi(u) = \rho e^{(u-u_{\text{th}})/\Delta u}$ ; no reset after spike emission	
E Synapse model		
<b>Plasticity</b>	Error-driven with continuous update (Eq. 4, Eq. 6)	
F Simulation Parameters		
<b>Populations</b>	$N = 5$	
<b>Connectivity</b>	$w_{\min} = -20, w_{\max} = 20, w_{\text{shift}} \sim \{-15, 15\}, w_0 = 5$	
<b>Neuron model</b>	$\rho = 0.2 \text{ Hz}, \Delta u = 1.0 \text{ mV}, E_L = -70 \text{ mV}, u_{\text{th}} = -55 \text{ mV}, \tau_m = 10 \text{ ms}, C_m = 250 \text{ pF}, \tau_s = 2 \text{ ms}$	
<b>Synapse model</b>	$\eta = 1.7, d = 1 \text{ ms}$	
<b>Input</b>	$r_{\min} = 150 \text{ Hz}, r_{\max} = 850 \text{ Hz}, T = 10,000 \text{ ms}, n_{\text{exp}} = 15$	
<b>Other</b>	$h = 0.01 \text{ ms}, \delta t = 5 \text{ ms}$	
G CGP Parameters		
<b>Population</b>	$\mu = 4, p_{\text{mutation}} = 0.045$	
<b>Genome</b>	$n_{\text{inputs}} = 3, n_{\text{outputs}} = 1, n_{\text{rows}} = 1, n_{\text{columns}} = 12, l_{\max} = 12$	
<b>Primitives</b>	Add, Sub, Mul, Div, Const(1.0)	
<b>EA</b>	$\lambda = 4, n_{\text{breeding}} = 4, n_{\text{tournament}} = 1$	
<b>Other</b>	max generations = 1000, minimal fitness = 0.0	

Table 2: Description of the network model used in the error-driven learning task (Sec. 4.6) (according to Nordlie et al., 2009).

A Model summary		
<b>Populations</b>	2	
<b>Topology</b>	—	
<b>Connectivity</b>	Feedforward with all-to-all connections	
<b>Neuron model</b>	Leaky integrate-and-fire (LIF) with delta-shaped post-synaptic currents	
<b>Plasticity</b>	Correlation-driven	
<b>Measurements</b>	Spikes, membrane potentials	
B Populations		
Name	Elements	Size
Input	Spike generators with pre-defined spike trains (see Sec. 4.7)	$N$
Output	LIF neuron	1
C Connectivity		
Source	Target	Pattern
Input	Output	All-to-all; synaptic delay $d$ ; initial weights chosen to yield an approximate initial firing rate of 20 Hz in the output neuron $w = \frac{u_{\text{th}}}{(N\nu - 2\sqrt{N\nu})/(10^{-3}\tau_m)}$
D Neuron model		
<b>Type</b>	LIF neuron with delta-shaped post-synaptic currents	
<b>Subthreshold dynamics</b>	$\frac{du}{dt} = -\frac{u - E_L}{\tau_m} + \frac{I_s(t)}{C_m}$ if $(t > t^* + \tau_r)$ $u(t) = u_r$ else	
<b>Spiking</b>	$I_s(t) = \sum_{i,k} w_k \delta(t - t_i^k)$ $k$ : neuron index, $i$ : spike index If $u(t-) < \theta \wedge u(t+) \geq \theta$ 1. set $t^* = t$ , 2. emit spike with time stamp $t^*$	
E Synapse model		
<b>Plasticity</b>	Correlation-driven (Eq. 12, Eq. 14, Eq. 15)	
F Simulation parameters		
<b>Neuron model</b>	$u_r = 0.0$ mV, $E_L = 0.0$ mV, $u_{\text{th}} = 20.0$ mV, $\tau_m = 18.0$ ms	
<b>Synapse model</b>	$d = 1.0$ ms, $W_{\text{max}} = 1.0$ mV, $\tau = 20.0$ mV, $\eta = 0.01$	
<b>Experiment</b>	$N = 1000$ , $T = 100$ s, $T_{\text{pattern}} = 100.0$ ms, $T_{\text{inter}} = 400.0$ ms, $\nu = 3.0$ Hz, $n_{\text{exp}} = 8$	
F CGP parameters		
<b>Population</b>	$\mu = 8$ , $p_{\text{mutation}} = 0.05$	
<b>Genome</b>	$n_{\text{inputs}} = 2$ , $n_{\text{outputs}} = 1$ , $n_{\text{rows}} = 1$ , $n_{\text{columns}} = 5$ , $l_{\text{max}} = 5$	
<b>Primitives</b>	Add, Sub, Mul, Div, Pow, Const(1.0)	
<b>EA</b>	$\lambda = 8$ , $n_{\text{breeding}} = 8$ , $n_{\text{tournament}} = 1$	
<b>Other</b>	max generations = 2000, minimal fitness = 10.0	

Table 3: Description of the network model used in the correlation-driven learning task (Sec. 4.7) (according to Nordlie et al., 2009).